

## Synthesis and Electrochemical Performance of Polypyrrole at High Scan Rates

Komal Khati, Ila Joshi, Anjali Bisht, M.G.H.Zaidi

Department of chemistry, G.B. Pant University of Agriculture & Technology, Pantnagar, Uttarakhand-263 145, India

---

**Abstract:** A novel attempt to synthesize Polypyrrole (PPY) through cationic surfactant Cetyltrimethylammonium bromide (CTAB) assisted in situ polymerization method. The structure and properties of PPY have been evaluated through analytical methods based on Fourier transform infrared spectra and simultaneous thermo gravimetric analysis reveals the formation of Polypyrrole. Sulphonated Polysulphone binded electrodes over 316 stainless steel substrate were fabricated and the supercapacitance ( $C_s$ ) of PPY has been evaluated with reference to Ag/AgCl through Cyclic Voltammetry (CV) at scan rates (V/s) ranging 0.05–0.2 in KOH (1.0M). A regular increase in  $C_s$  has been observed irrespective to scan rates. PPY shows  $C_s$  36.01(F/g) at a scan rate of 0.05 V/s. The cyclic stability of the PPY with decrease in capacitive behavior during the first 50 cycles at a scan rate of 0.1 V/s. The corrosion performances of the PPY coating were investigated by AC impedance spectroscopy. It was seen that bare steel coated PPY film provided better protection for long exposure times in KOH (1.0M) solution.

**Keywords:** Cetyltrimethylammonium bromide, Cyclic Voltammetry, Electrochemical performance, Polypyrrole, Supercapacitor.

---

### I. Introduction

Electrochemical supercapacitors, also known as electrochemical capacitors, are capacitors with capacitance values greater than any other capacitor type available today, they utilize high surface area electrode materials and thin electrolytic dielectrics to achieve capacitances several orders of magnitude larger than conventional capacitors **Choi et al., 2015**. Electrical double layer capacitors (EDLCs) are one of the promising electrochemical energy storage devices with high power characteristics. In this context, among various conducting polymers, PPY has received increasing attention as electroactive material for energy storage devices (EEDs) because of their ability to dramatically change properties when stimulated by an electrical signal offer exciting prospects for development of a wide range of new EEDs such as electrochemical supercapacitors and batteries **Stejskal et al., 2014**.

The flexible electrodes have important potential applications in energy storage of portable electronic devices for their powerful structural properties. Recently, several kinds of conductive polymers were investigated for development of the flexible electrodes for electrochemical supercapacitors. This has been the focus of a great deal of R & D and applications of supercapacitors because of high electrical conductivity of the conducting polymers in doped state, high specific or electrochemical capacitance ( $C_s$ ), good chemical and thermal stability, environmental friendly properties and facile synthesis **Kim et al., 2006, Jiang et al., 2009**.

The need of the development of a polymer for conservation and storage of electrochemical energy EEDs, in the present work, efforts were made to synthesize PPY through CTAB assisted in situ polymerization method in presence of ferric chloride. All such synthesized materials were characterized through spectra, based on FT-IR and TGA. The electrochemical behavior of the synthesized material and their supercapacitance has been investigated through CV in KOH to ascertain their potentials as EEDs **Mudila et al., 2013**.

### II. Materials and Method

The monomer Pyrrole (PY) was purchased from Acros Chemicals, Cetyltrimethylammonium bromide (>99 %) was procured from Sigma Aldrich. Rest of the chemicals and solvents were purchased from Sd Fine Chemicals, India and used without further purification. Sulfonated Polysulphone (SPS) was prepared through Chlorosulfonation of polysulphone **Goel et al., 2011**. Prior to polymerization reactions, PY was dried with NaOH and fractionally distilled under reduced pressure from  $\text{CaH}_2$  and stored at 4 °C.

#### 2.1 Synthesis of Polypyrrole

Polypyrrole was synthesized by cationic surfactant assisted dilute polymerization method. In this process, a suspension of monomer (0.12 M) in de-ionized water stabilized with CTAB (1.145 g) was placed in a thermostatically controlled glass reactor assembly comprising three necked flask equipped with mechanical stirrer, thermometer and a dropping funnel. The contents were stirred @ 500 rpm over 15 min at  $30 \pm 1$  °C.

Meanwhile, the dropping funnel was charged with ferric chloride ( $\text{FeCl}_3$ ) solution (50 mL,  $1.85 \times 10^{-2}$  mol/dL). The process of polymerization was initiated through dropwise addition of solution of  $\text{FeCl}_3$  to the CTAB stabilized monomer. The polymerization process was identified by the black colour of the reaction mixture. The polymerization process was allowed to progress @ 500 rpm over 24 h at  $30 \pm 1^\circ\text{C}$ , where polymer was precipitated. Polymer was collected through filtration and successively washed with de-ionized water until colourless filtrate was obtained. The obtained polymer in the form of powder was dried at  $60 \pm 1^\circ\text{C}/400$  mm Hg over 8 hours.

## 2.2 Preparation of working electrodes

The commercially available 316 Stainless Steel (SS) was cut into  $1\text{cm}^2$  area and finished with an emery paper (mesh size 320600). It was then de-greased with acetone and subjected to surface oxidation at  $50 \pm 1^\circ\text{C}$  for 1h. The requisite proportions of electroactive material (65 mg) along with graphite (10 mg) were added to a solution of SPS (5g/dL) in N-methyl Pyrrolidone (NMP). The contents were ultrasonicated for 20 minutes. The solution (50 $\mu\text{L}$ ) was applied over SS substrate. The electrodes were left overnight at ambient temperature, followed by  $50^\circ\text{C}/400$  mm Hg for 48 hours. The final mass thickness of the electroactive materials was achieved to  $0.05 \pm 0.01$  mg over 316-SS substrate and used for all the electrochemical characterizations (Mudila *et al.*, 2013).

## 2.3 Characterization

Fourier transform Infra-red (FT-IR) spectra of samples were recorded on Perkin Elmer spectrophotometer in KBr, from  $4000$  to  $400\text{ cm}^{-1}$  on transmission mode. Thermo-oxidative stability of samples was investigated at sample size (mg) ranging 8.08-10.02 through simultaneous thermo gravimetric analysis under  $\text{N}_2$  atmosphere over EXSTAR TG/DTA 6300 instrument in static air at a heating rate of  $10^\circ\text{C}/\text{minute}$  up to  $600^\circ\text{C}$  using alumina powder as reference.

## 2.4 Electrochemical Characterization

### 2.4.1 Evaluation of supercapacitance

The electrochemical characterization of electroactive material was carried out in a 1.0 M KOH solution using an electrochemical workstation (IVIUM Potentiostat- Galvanostat Netherlands BV) in a three electrode cell assembly with reference to (Ag/AgCl) electrode. Pt foil with  $1\text{ cm}^2$  area was used as counter electrode and the prepared electrodes were served as a working electrode. CV was conducted over a current compliance 1mA and ranges of voltage compliance  $-0.6$  to  $-0.1\text{V}$  at scan rate (V/s) 0.05 to 0.2. All the measurements were performed at ambient temperature. Specific capacitance (Cs) of the active material were calculated from the voltammetric charges by the CV curve, by means of relation

$$Cs = \frac{qa + |qc|}{2m\Delta V}$$

where "qa" and "qc" are the voltammetric charges on anodic and cathodic scans, respectively in the capacitive potential region ( $\Delta V$ ) and "m" being the mass of active material.

Electrochemical impedance spectroscopy (EIS) was performed to determine the parameters for electron transfer reactions at the interface of the working electrode in the KOH solution (1.0M). An alternating voltage of amplitude 0.03 V with sweeping frequencies between 1000 Hz to 0.1 Hz was coupled to a frequency response analyzer (FRA) to acquire Nyquist plots, @ 4 points per decade change in frequency. The EIS results were confirmed by measurements of sample at intervals from 0 to 32 hrs immersion.

## III. Results and Discussion

### 3.1 FT-IR spectra

In (Fig.1) PPY shows characteristics FT IR absorptions ( $\text{cm}^{-1}$ ) corresponding to N-H (3421.65) Jiwei *et al.*, 2010, mC-H (2,917.67), m symmetrical C=C (1,652.10), m C-C (1,463.2), mC-N (1,513.20) Sonavane *et al.*, 2010, mC=C (1,545.37) representing the formation of 2,5-substituted PPY Qiao *et al.*, 2010, C-H in-plane deformation (1,376.09) Arora *et al.*, 2006 and peaks at  $675.51\text{ cm}^{-1}$  corresponding to ring deformation,  $912\text{ cm}^{-1}$  corresponding to C-H deformation, Doping induced bands associated with conjugated backbone for PPY appeared at 1,160.40 Zhao *et al.*, 2011. Sharp peaks at 2,360.42 correspond to m O-H due to the formation of oxidized PPY Tian and Zerbi, 2009, Chougulea *et al.*, 2011.

### 3.2 Thermo-oxidative stability

Fig.2 shows thermogram of PPY. Thermal decomposition of materials was investigated at  $100^\circ\text{C}$  corresponding to moisture content associated with material and the range of major wt loss in terms of TG onset and TG endset. The thermo-oxidative degradation of PPY has been expressed in terms of their TG weight loss (% w/w) with reference to decomposition temperature ( $^\circ\text{C}$ ) curves reveal the hygroscopic nature of PPY due to their respective weight loss of 8.07 below  $100^\circ\text{C}$  arises mainly from the expulsion of moisture Emma *et al.*,

**2007.** Thermal decomposition of PPY starts at TG onset temperature ( $^{\circ}\text{C}$ ) 300 leaving residue (%) 72.25. Prior to TG onset increase in temperature ( $^{\circ}\text{C}$ ) at 200 has left wt residue  $W_L$  (%) 86.96. PPY shows TG endset temperature ( $^{\circ}\text{C}$ ) at 591 leaving char residue (%) -1.20 (**Basavaraja *et al.*, 2009**).

### 3.3 Electrochemical Behavior

The electrochemical behavior of PPY has clearly been indicated through cyclic voltammetry (Fig.3a). Cyclic voltammetry technique to determine the electrochemical performance of PPY electrode measured in 1.0 M KOH solution at a scan rate ranging 0.05 -0.2 mV/s in a potential window of -0.6 to -0.1V. With scan rate, a regular increase in the peak currents has been observed for PPY in the potential range -0.6 to -0.1. The calculations based on I/V characteristics reveals  $C_s$  (F/g) of PPY 36.01–14.88 (Fig.3b). Voltammogram reveals a regular increase in the ranges of cathodic and anodic currents with scan rate with a capacitive decrease of  $\sim 1\%$  during the first 50 cycles at a scan rate of 0.1 V/s, indicating the excellent cyclic stability for supercapacitor applications (Fig.3c).

The AC impedance response of electrode is shown in (Fig. 4). For the electrode and the capacitor, a semicircle is obtained at high frequency and a straight line in the low-frequency region. The capacitance values increase at low frequencies due to a larger number of ions moving which cause a decrease in the bulk resistance of the capacitor. In the low frequency region, the linear region more towards imaginary axis and this indicates good capacitive behavior **Zhang *et al.*, 2011**.

### 3.4 Potentiodynamic Polarization Measurements

The Tafel plot analysis give information about the extent of corrosion inhibition ability of the composite coating by measuring corrosion potential ( $E_{\text{corr}}$ ), corrosion current density ( $I_{\text{corr}}$ ) and corrosion rate (CR) associated with polarization measurements of the sample. The corrosion protection behavior of bare steel and PPY coated steel in a corrosive medium (1.0M KOH) under potentiodynamic polarization conditions is presented in (Fig.5) depicts the polarization behaviour of bare steel electrode with PPY coating plotted from -1.0V to 1.0V at scan rate of 0.1V/s after immersion in 1.0M KOH at room temperature with their stable OCP values respectively. The electrochemical parameters corrosion current ( $I_{\text{corr}}$ ), corrosion potential ( $E_{\text{corr}}$ ) calculated from Tafel plots for PPY. The tested free-standing film used for the molecular barrier measurements was prepared with a thickness of 0.05 mm. The more negative  $E_{\text{corr}}$  and the larger  $I_{\text{corr}}$  usually correspond to faster corrosion rates while the more positive  $E_{\text{corr}}$  and the smaller  $I_{\text{corr}}$  mean a slower corrosion process. Extrapolation of anodic and cathodic tafel lines is one of the most popular AC techniques for charge transfer controlled reactions estimating the corrosion rate.

It was observed from the polarization curve (Fig.5) at scan rate 0.1 V/s the bare steel denotes a sudden increase of the current at anodic branch exhibiting a passivity region which is attributed to the formation of a protective oxide layer. From the results it is clear that corrosion potential ( $E_{\text{corr}}$ ) of bare steel is -1.27 V with higher current density  $I_{\text{corr}} 1.90 \times 10^{-4}$  (A/cm<sup>2</sup>) at 0.1 V/s in KOH solution **Chang *et al.*, 2012**.

The PPY coating shows  $E_{\text{corr}} -1.07$  V and  $I_{\text{corr}} 4.02 \times 10^{-4}$  (A/cm<sup>2</sup>) at scan rate 0.1 V/s confirming the protective behavior of coating towards bare steel. Thus PPY exhibited the anti-corrosion capability as evidenced by the highest and lowest values of  $E_{\text{corr}}$  and  $I_{\text{corr}}$  **Mondal *et al.*, 2014**.

IV. Figures and Table

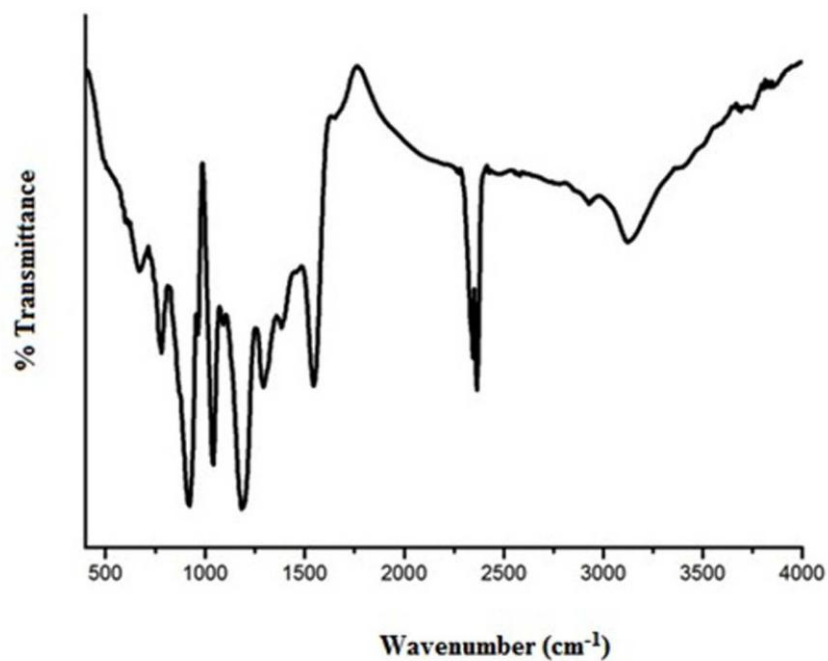


Figure-1  
FT-IR spectra of Polypyrrole

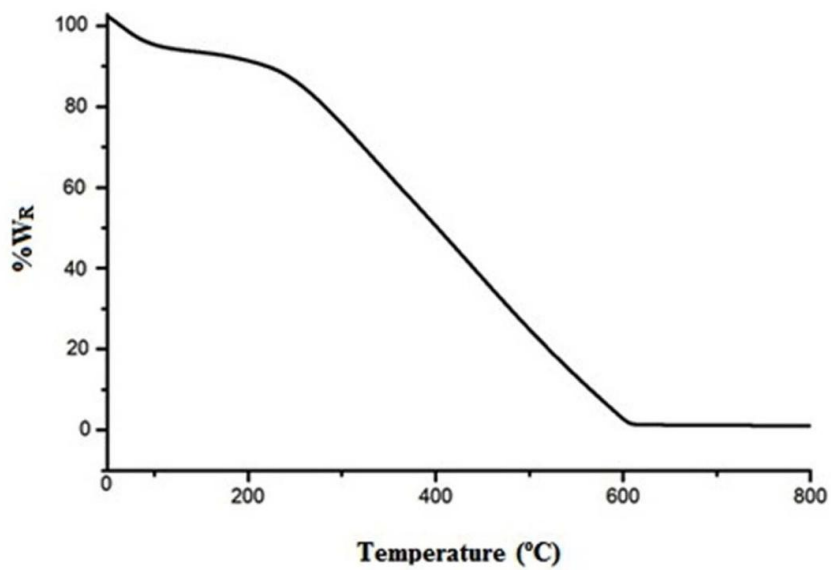


Figure-2  
TGA curve of Polypyrrole

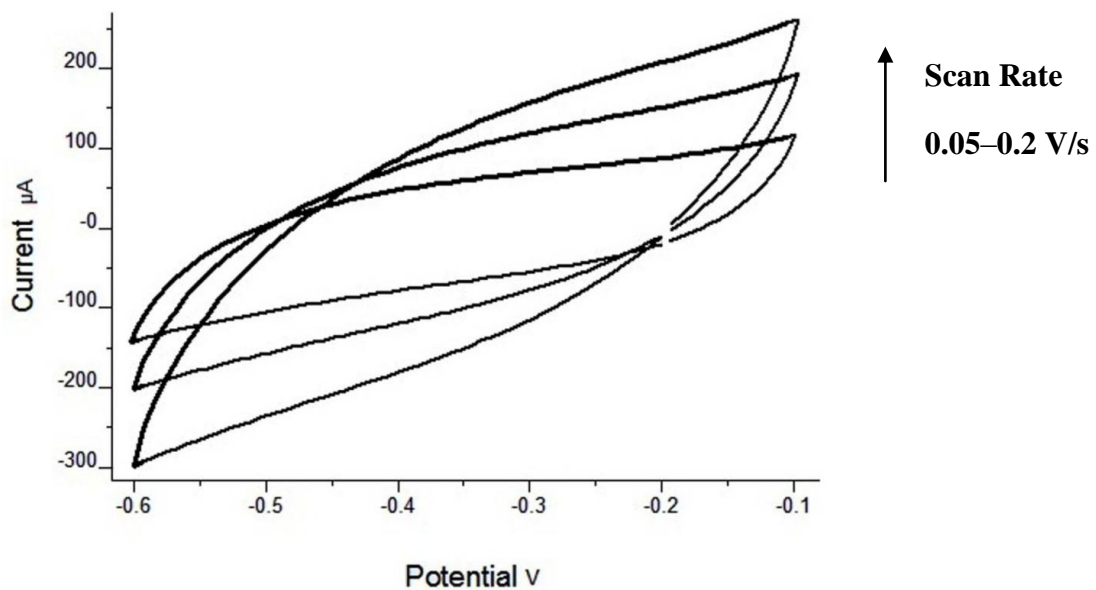


Figure-3(a)  
CV of PPY at Various Scan Rate

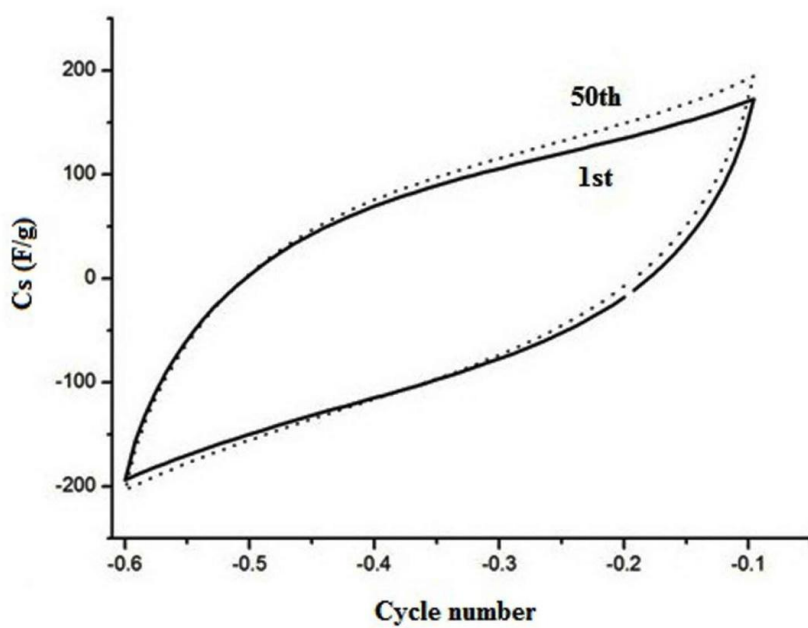


Figure-3(b)  
CV of PPY at 0.1 V/s Upto 50 Cycle

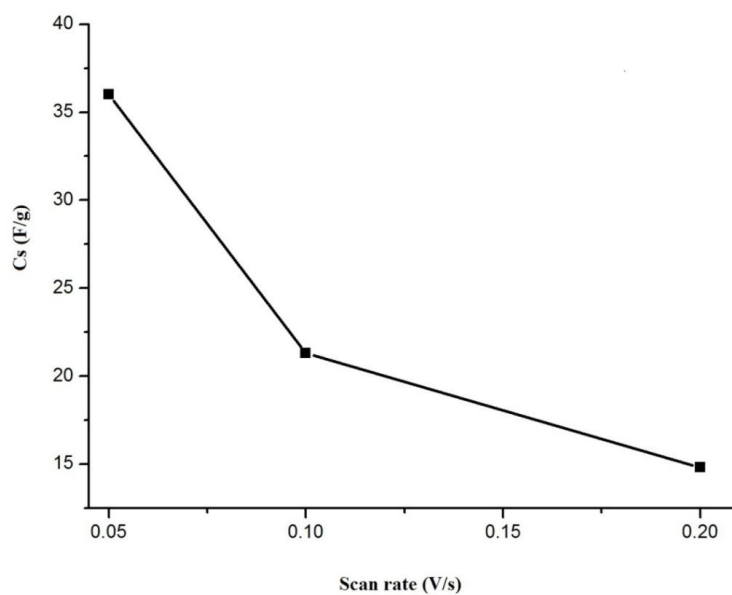


Figure-3(c)  
Effect of Scan Rate on Cs of PPY

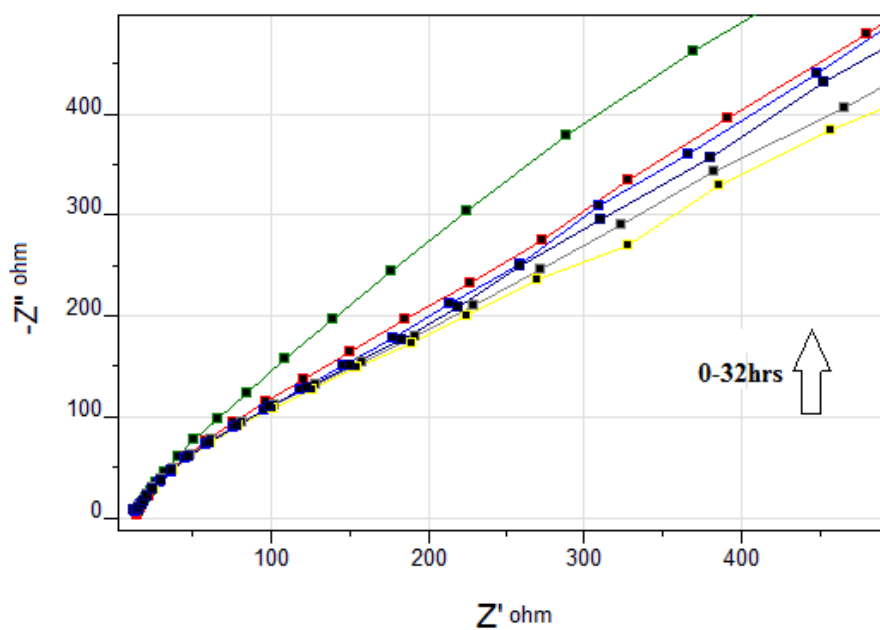
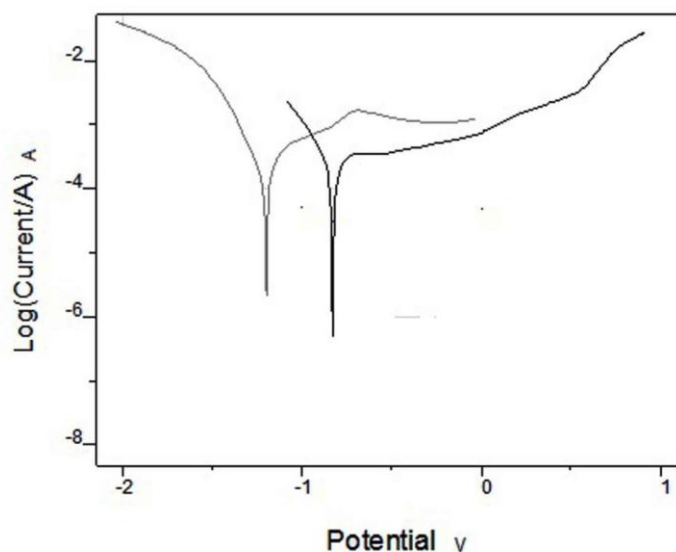


Figure-4  
Fig. 4. Nyquist impedance plots of the PPY electrodes



**Figure-5**  
**Tafel plot @0.1 V/s (Grey-bare steel, Black-PPY) in KOH**

### V. Conclusion.

A process was developed to synthesize Polypyrrole. The process involved cationic surfactant assisted in situ polymerization method for electrochemical supercapacitor applications. Diversified studies of PPY are fully characterized by different techniques such as FT-IR and TGA confirmed the formation of electroactive polymer. The electrochemical behavior of PPY has been investigated through cyclic voltammetry at higher scan rates (V/s) ranging 0.05–0.2 in KOH (1.0M). A regular increase in specific capacitances was achieved by Polypyrrole. The specific capacitance  $C_s$  (F/g) of PPY 36.01 at a scan rate 0.05 V/s. The electrochemical studies revealed that PPY can be used as a promising electrode material for the supercapacitor. The corrosion performance of bare steel coated PPY was investigated by using electrochemical impedance spectroscopy in alkaline medium. Tafel plot revealed an excellent material used for corrosion protection.

### Acknowledgements

The financial assistance granted by CSIR-UGC fellowship is acknowledged.

### References

- [1]. Choi, H. and Yoon, H. Nanostructured Electrode Materials for Electrochemical Capacitor Applications, *Nanomaterials*, 5: 2015, 906-936.
- [2]. Stejskal, J.; Bober, P.; Trchova, M.; Horsky, J.; Pilar, J. and Walterova, Z. The oxidation of aniline with p-benzoquinone and its impact on the preparation of the conducting polymer, polyaniline. *Synth. Met.* 192: 2014, 66 -73.
- [3]. Kim, H.; Lee, Y.S.; Sharma, A.K. and Liu, C.G. Polypyrrole/Carbon Composite Electrode for High- Power Electrochemical Capacitors, *Electrochimica Acta*. 52: 2006, 1727-1732.
- [4]. Jiang, J.; Zhang, L.; Wang, X.; Holm, N.; Rajagopalan, K.; Chen, F. and Ma, S. Highly ordered macroporous woody biochar with ultra-high carbon content as supercapacitor electrodes, *Electrochimica Acta*, <http://dx.doi.org/10.1016/j.electacta.2013.09.121>.
- [5]. Goel, S.; Mazumdar, N. A. and Gupta, A. J. *Nanosci.Nanotechnol.*, 11(11): 2011, 10164–10172.
- [6]. Mudila, H.; Rana, S.; Zaidi, M.G.H. and Alam, S. Fullerenes, Nanotubes and Carbon Nanostructures, DOI:10.1080/1536383X.2013.787604 .
- [7]. Emma, J.; Erika, M.; Ma'riahermal, O. Decomposition of polypyrroles, *J. Therm. Anal. Cal.*, 88: 2007, 515–521.
- [8]. Zhang, D.; Zhang, X.; Chen, Y.; Yu, P.; Wang, C. and Ma, Y. Enhanced capacitance and rate capability of graphene/polypyrrole composite as electrode material for supercapacitors, *Journal of Power Sources*, 196, 2011, 5990–5996.
- [9]. Mondal, J.; Marandi, M.; Kozlova, J.; Merisalu, M.; Niilisk, A. and Sammelselg, V., Protection and Functionalizing of Stainless Steel Surface by Graphene Oxide-Polypyrrole Composite Coating, *Chem. Chem. Eng.*, 8: 2014,786-793.
- [10]. Tian, B. and Zerbi, G. Lattice-Dynamics and Vibrational-Spectra of Polypyrrole, *Journal of Chemical Physics*, 92: (6), 2009,3886-3891.doi:10.1063/1.457794.
- [11]. Chougulea, A. M.; Pawara, G. S.; Prasad, R. G.; Mulika, N. R.; Sen, S. and Patila, B. V. Synthesis and Characterization of Polypyrrole(PPy) Thin Films, *Soft Nanoscience Letters*, 1: 2011,6-10.
- [12]. Arora, K.; Chaubey, A.; Singhal, R.; Singh, P. R.; Pandey, K. M.; Samanta, B. S.; Malhotra, D. B. and Chand, S. Application of Electrochemically Prepared Polypyrrole- Polyvinyl Sulphonate Films to DNA Biosensor, *Biosensors and Bioelectronics*, 21:( 9), 2006,1777-1783.
- [13]. Jiwei, L.; Jingxia, Q.; Miao, Y. and Chen, J. *J. Mater. Sci.*, 43: 2008, 6285–6288.
- [14]. Qiao, Y.S.; Shen, L.Z.; Dou, T. and Huc, M. *Chin. J. Polym. Sci.*, 28: 2010, 923–93.
- [15]. Zhao, Y.; Zhan, L.; Tian, J.; Nie, S. and Ning, Z. *Electrochim. Acta*, 56: 2011, 1967–1972.
- [16]. Basavaraja, C.; Kim, N. R.; Joe. A.; Pierson, R.; Huh, D. S. and Venkataraman, A. *Korean Chem. Soc.*, 30(11): 2009, 2701.
- [17]. Chang, C.H.; Huang, T.C.; Peng, C.W.; Yeh, T. C.; Lu, H. I.; Hung, W.I.; Weng, C.J.; Yang, T.I. and Yeh, J. M. 2012. Novel anticorrosion coatings prepared from polyaniline/graphene composites, *Carbon*, 50: 5044–5051.